

See discussions, stats, and author profiles for this publication at: <https://www.researchgate.net/publication/262566016>

# X-ray Birefringence: A New Strategy for Determining Molecular Orientation in Materials

ARTICLE *in* JOURNAL OF PHYSICAL CHEMISTRY LETTERS · OCTOBER 2012

Impact Factor: 7.46 · DOI: 10.1021/jz3013547

CITATIONS

5

READS

30

9 AUTHORS, INCLUDING:



**Benjamin Alexander Palmer**

Weizmann Institute of Science

20 PUBLICATIONS 43 CITATIONS

SEE PROFILE



**Benson Kariuki**

Cardiff University

348 PUBLICATIONS 5,032 CITATIONS

SEE PROFILE



**Gin Keat Lim**

Universiti Sains Malaysia

14 PUBLICATIONS 99 CITATIONS

SEE PROFILE



**Igor P Dolbnya**

Diamond Light Source

127 PUBLICATIONS 1,880 CITATIONS

SEE PROFILE

# X-ray Birefringence: A New Strategy for Determining Molecular Orientation in Materials

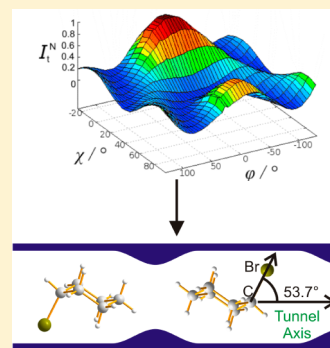
Benjamin A. Palmer,<sup>†</sup> Gregory R. Edwards-Gau,<sup>†</sup> Anabel Morte-Ródenas,<sup>†</sup> Benson M. Kariuki,<sup>†</sup> Gin Keat Lim,<sup>‡</sup> Kenneth D.M. Harris,<sup>\*,†</sup> Igor P. Dolbnya,<sup>‡</sup> and Stephen P. Collins<sup>‡</sup>

<sup>†</sup>School of Chemistry, Cardiff University, Park Place, Cardiff CF10 3AT, Wales

<sup>‡</sup>Harwell Science and Innovation Campus, Diamond Light Source, Didcot, Oxfordshire OX11 0DE, England

**ABSTRACT:** While the phenomenon of birefringence is well-established in the case of visible radiation and is exploited in many fields (e.g., through the use of the polarizing optical microscope), the analogous phenomenon for X-rays has been a virtually neglected topic. Here, we demonstrate the scope and potential for exploiting X-ray birefringence to determine the orientational properties of specific types of bonds in solids. Specifically, orientational characteristics of C–Br bonds in the bromocyclohexane/thiourea inclusion compound are elucidated from X-ray birefringence measurements at energies close to the bromine K-edge, revealing *inter alia* the changes in the orientational distribution of the C–Br bonds associated with a low-temperature order–disorder phase transition. From fitting a theoretical model to the experimental data, reliable quantitative information on the orientational properties of the C–Br bonds is determined. The experimental strategy reported here represents the basis of a new approach for gaining insights into the orientational properties of molecules in anisotropic materials.

**SECTION:** Surfaces, Interfaces, Porous Materials, and Catalysis



The phenomenon of optical birefringence<sup>1</sup> (which arises from the dependence of refractive index on the orientation of an anisotropic material with respect to the plane of polarization of incident light) is very well established and underpins the powerful and wide-ranging applications of the polarizing optical microscope in many scientific fields.<sup>2,3</sup> Thus, while the interaction of linearly polarized visible light with solids is widely exploited, the opportunity to utilize the phenomenon of birefringence in the case of linearly polarized X-rays<sup>4–7</sup> has remained remarkably neglected. Indeed, the first definitive demonstration of X-ray birefringence was only reported very recently<sup>7</sup> and focused on a model material that was shown to exhibit essentially ideal birefringence behavior at X-ray energies near the Br K-edge. The designed material (the 1-bromoadamantane/thiourea inclusion compound<sup>8</sup>) gave experimental behavior in excellent agreement with theoretical predictions for the dependence of transmitted X-ray intensity on both X-ray energy and crystal orientation for the case of a material in which all C–Br bonds are aligned strictly parallel to each other and with a *known* orientation of the C–Br bonds relative to the crystal axes. However, given the strong interdependence between X-ray birefringence and the orientational characteristics of specific bonds in materials, there is considerable potential to exploit measurements of X-ray birefringence to establish insights into bond orientational properties for cases in which the bond orientations are *unknown* or poorly characterized (e.g., in the case of disordered materials).

In this Letter, we report the first demonstration of a strategy for exploiting X-ray birefringence to determine the orientational

properties of molecules in solids, specifically by applying this technique to investigate changes in bond orientations associated with orientational ordering processes as a function of temperature. We focus on the bromocyclohexane/thiourea (BrCH/thiourea) inclusion compound and explore the potential for X-ray birefringence to reveal temperature-dependent changes in the orientational properties of the C–Br bonds of the BrCH guest molecules.

Structural and dynamic properties of the BrCH/thiourea inclusion compound have been studied previously by single-crystal and powder XRD,<sup>9,10</sup> solid-state NMR,<sup>11–15</sup> and other techniques.<sup>16,17</sup> At ambient temperature, BrCH/thiourea has the “conventional” rhombohedral host structure of thiourea inclusion compounds<sup>18–21</sup> (Figure 1a), comprising tunnels within which the BrCH guest molecules are located. At ambient temperature, the BrCH guest molecules (and thus the C–Br bonds) undergo unrestricted reorientation within the tunnel, giving rise to essentially isotropic disorder. At 233 K, the material undergoes a first-order phase transition,<sup>10,14</sup> at which the rhombohedral thiourea host structure of the high-temperature (HT) phase distorts to a monoclinic structure<sup>10</sup> in the low-temperature (LT) phase (Figure 1b) while retaining the same hydrogen-bond connectivity.

The aim of the present research is to exploit measurements of X-ray birefringence to gain insights into the orientational characteristics of the C–Br bonds of the BrCH guest molecules

**Received:** September 5, 2012

**Accepted:** October 10, 2012

**Published:** October 10, 2012



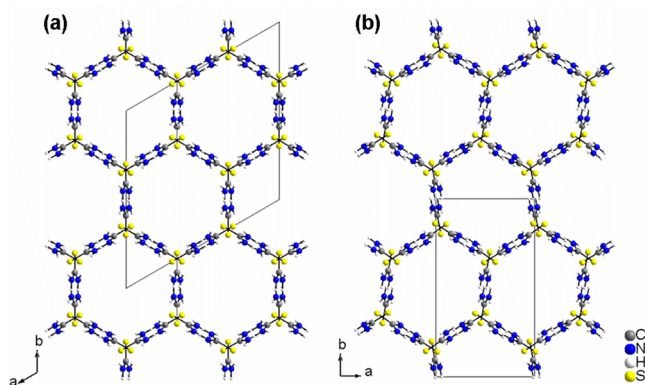


**Figure 1.** (a) The “conventional” rhombohedral thiourea host structure, as observed in the HT phase of BrCH/thiourea, viewed along the tunnel axis. In this phase, the guest molecules (not shown) are isotropically disordered. (b) The thiourea host structure of BrCH/thiourea in the LT phase at 110 K (the distortion of the host tunnel relative to the HT phase is clearly seen).

in BrCH/thiourea, both in the HT and LT phases, and particularly to resolve the temperature dependence of the orientational distribution of the C–Br bonds within the LT phase. Quantitative information relating to the orientational distribution of the C–Br bonds is established by fitting the experimental X-ray birefringence data using a theoretical model developed in this Letter.

To study X-ray birefringence, the transmission of linearly polarized X-rays through a single crystal of BrCH/thiourea<sup>22</sup> was studied in the “crossed polarizer” geometry shown in Figure 2a, with incident X-ray energy near the Br K-edge. In our experimental setup, the tunnel axis (*c*-axis) of the crystal was maintained in the plane (*xy*-plane) perpendicular to the direction of propagation of the incident X-ray beam (*z*-axis),

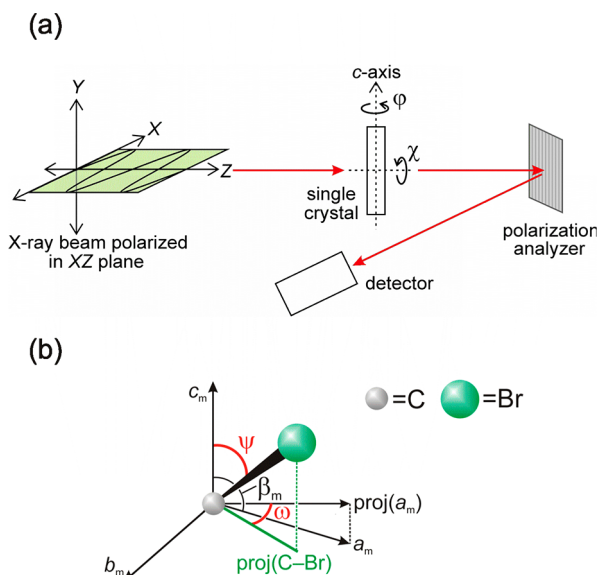


**Figure 2.** (a) Schematic of the experimental setup for measurement of X-ray birefringence. The incident X-ray beam is propagated along the *z*-axis and is linearly polarized along the *x*-axis. The crystal orientation angles  $\chi$  and  $\varphi$  are defined. (b) Schematic of the BrCH/thiourea crystal defining the bond tilt angle  $\psi$  and the bond azimuthal angle  $\omega$  for the C–Br bond of the BrCH guest molecule relative to the crystallographic axes of BrCH/thiourea in the monoclinic LT phase.

with the incident beam linearly polarized along the *x*-axis (horizontal). The crystal orientation was varied by rotation about the angles  $\chi$  and  $\varphi$  defined in Figure 2a, where  $\chi$  refers to rotation of the *c*-axis of the crystal around the laboratory *z*-axis and  $\varphi$  refers to rotation of the crystal around the *c*-axis. The *c*-axis is the tunnel axis of the thiourea host structure in both the HT and LT phases. With respect to the hexagonal unit cell ( $a_h, b_h, c_h$ ) of BrCH/thiourea in the HT phase, in the orientation with  $\chi = 0^\circ$  and  $\varphi = 0^\circ$ , the  $c_h$ -axis is parallel to the *x*-axis (and hence lies in the horizontal *xz*-plane), and the (100) plane is perpendicular to the *z*-axis. With respect to the monoclinic unit cell ( $a_m, b_m, c_m$ ) of the LT phase, in the orientation with  $\chi = 0^\circ$  and  $\varphi = 0^\circ$ , the  $c_m$ -axis is parallel to the *x*-axis (in the horizontal plane), the  $b_m$ -axis is parallel to the *z*-axis, and the projection of the  $a_m$ -axis onto the plane perpendicular to the  $c_m$ -axis [denoted  $\text{proj}(a_m)$ ] is perpendicular to the *xz*-plane.

Measurements of X-ray birefringence using the experimental setup in Figure 2a were carried out on beamline B16 at the Diamond Light Source, employing a five-circle, vertical-scattering, Huber eulerian diffractometer. On beamline B16, the incident X-ray beam is highly linearly polarized in the horizontal plane, with the exact degree of linear polarization depending on the vertical beam size. In the present work, it is established from fitting the theoretical model to our X-ray birefringence data (discussed below) that the incident beam was 99% linearly polarized. The X-ray polarization analyzer was highly oriented pyrolytic graphite, which operates by means of Bragg diffraction close to  $2\theta = 90^\circ$ , and an avalanche photodiode counting detector was used. All measurements were carried out with the incident X-ray energy fixed at 13.493 keV, which corresponds to the midpoint of the bromine K-edge for BrCH/thiourea (established in the present work from X-ray absorption spectra recorded in the HT phase for BrCH/thiourea; in the HT phase, the bromine K-edge X-ray absorption spectrum is essentially independent of crystal orientation). The dimensions of the crystal were  $\sim 2$  mm along the tunnel axis of the thiourea host structure and  $\sim 0.5$  mm perpendicular to this axis. The dimensions of the focused X-ray beam were 0.3 mm (horizontal) and 0.3 mm (vertical).

At each temperature, the experimental data comprise measurements of transmitted X-ray intensity (denoted  $I_t$ ) as a function of the crystal orientation angles  $\chi$  and  $\varphi$ . To extract structural information, simulated data calculated for a theoretical model were fitted to the experimental data  $I_t(\chi, \varphi)$  using a least-squares procedure. More details of the model are given below.

For comprehensive studies of X-ray birefringence at a given temperature (results shown in Figure 3),  $I_t$  was measured as a function of crystal orientation ( $\chi, \varphi$ ), with  $\chi$  sampled from  $-25$  to  $95^\circ$  in steps of  $10^\circ$  and with  $\varphi$  sampled from  $-135$  to  $135^\circ$  in steps of  $5^\circ$ . The measurement time at each crystal orientation was 2 s. For the one-dimensional scans shown in Figure 4, the  $\chi$  scan (with  $\varphi$  fixed; Figure 4a) was carried out from  $\chi = -25$  to  $95^\circ$  in steps of  $2^\circ$ , with a measurement time of 5 s per step. The  $\varphi$  scan (with  $\chi$  fixed; Figure 4b) was carried out from  $\varphi = -135$  to  $135^\circ$  in steps of  $5^\circ$ , with a measurement time of 5 s per step.

All data reported here were recorded on the same single crystal of BrCH/thiourea and (with the exception of the results in Figure 6) were recorded on the first cooling cycle of the crystal from 270 to 100 K. The data in Figure 6 were recorded on warming the crystal<sup>23</sup> for the first time from 100 to 270 K. The entire set of measurements was repeated for a second

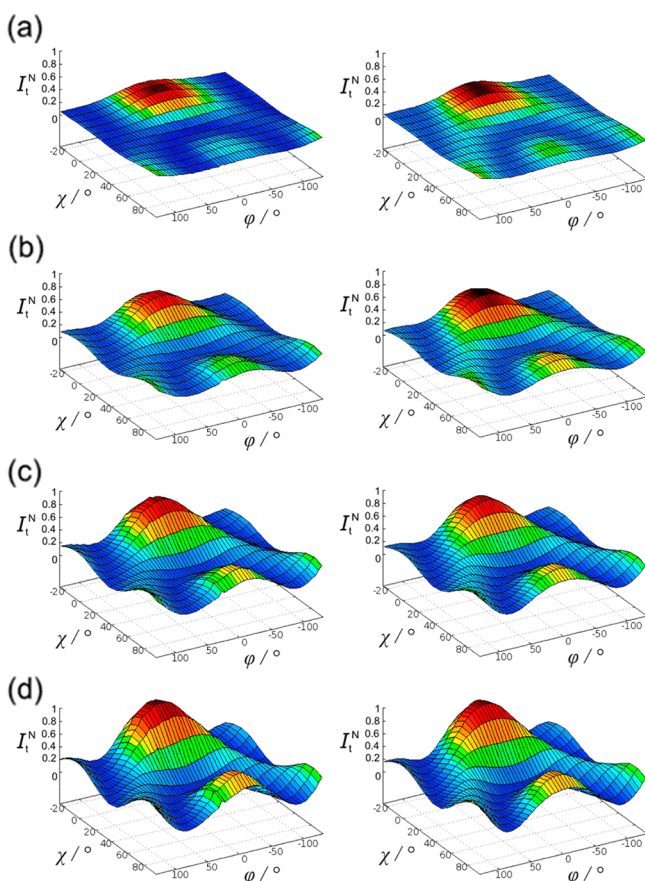


**Figure 3.** (Left) Experimental data of normalized transmitted X-ray intensity ( $I_t^N$ ) as a function of  $\chi$  and  $\phi$  for the experimental setup in Figure 2a at different temperatures: (a) 200 K, (b) 160 K, (c) 130 K, (d) 100 K. (Right) Best-fit simulated data, calculated using the structural model described in the text, at each temperature in the LT phase. The fitted parameters obtained in each case are shown in Table 1. The normalized transmitted intensities were calculated by scaling the measured transmitted intensities relative to the highest intensity recorded in the entire experiment (i.e., for the specific crystal orientation giving the highest transmitted intensity at 100 K).

cooling and warming cycle on the same crystal of BrCH/thiourea. No significant differences were observed in the X-ray birefringence behavior as a function of temperature between the first and second cooling/warming cycles (and no changes in behavior were observed as a function of X-ray beam exposure time).

The theoretical model for calculating  $I_t(\chi, \phi)$  data assumes that the crystal exhibits uniaxial anisotropy with the optic axis along the direction of the C–Br bond (thus, the model is applicable to a situation in which there is a single orientational domain of the BrCH guest molecules). The orientation of the C–Br bond relative to the crystallographic axes (in the LT phase) is specified by two angles defined in Figure 2b, the bond tilt angle (denoted  $\psi$ ) between the C–Br bond and the tunnel axis (the  $c_m$ -axis) and the bond azimuthal angle (denoted  $\omega$ ) between the projection of the C–Br bond on the plane perpendicular to the  $c_m$ -axis and the projection of the  $a_m$ -axis on this plane.

Although the model involves 11 parameters,<sup>24</sup> the values of several parameters are known and were fixed in the fitting procedure (see ref 24 for details). The parameters that potentially have a significant dependence on temperature are

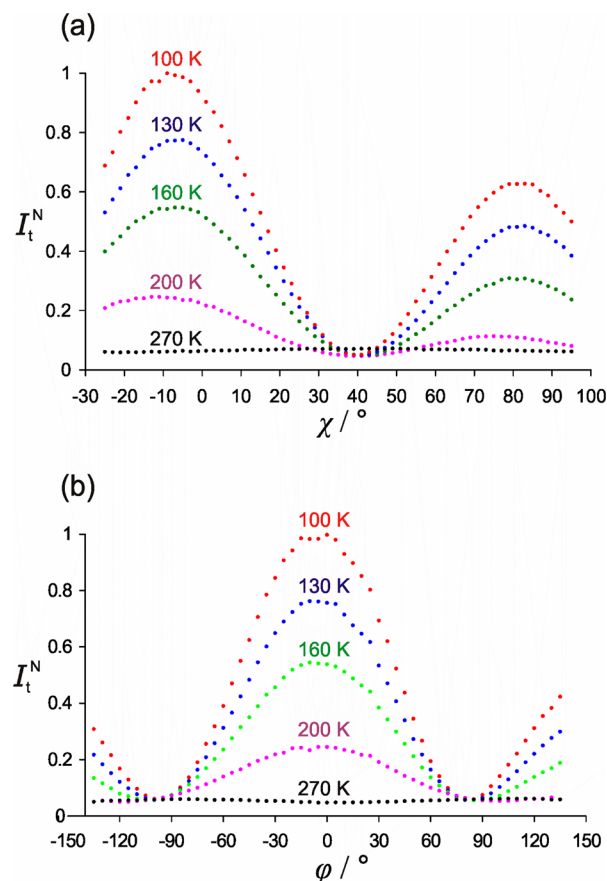


**Figure 4.** Normalized transmitted X-ray intensity ( $I_t^N$ ) for a single crystal of BrCH/thiourea (a) as a function of  $\chi$  with  $\phi$  fixed at  $0^\circ$  and (b) as a function of  $\phi$  with  $\chi$  fixed at  $-10^\circ$ . In both (a) and (b), data recorded at the following temperatures are shown: 270 (black), 200 (pink), 160 (green), 130 (blue), and 100 K (red).

the angles ( $\psi$  and  $\omega$ ) defining the orientation of the C–Br bond with respect to the crystallographic axes and the molecular polarization factor ( $p$ ). The parameter  $p$  quantifies the degree of polarization of the ensemble of BrCH guest molecules and can be considered as the resultant of the direction of all C–Br bonds in the material<sup>25</sup> ( $p$  acts as a prefactor for the complex anisotropic absorption coefficient). Thus,  $p$  will attain its maximum value ( $p = 1$ ) when all C–Br bonds in the material have the same orientation and will attain its minimum value ( $p = 0$ ) when there is isotropic disorder of the C–Br bonds.

In the least-squares fitting of the simulated data to the experimental data, the parameters  $p$ ,  $\psi$ , and  $\omega$  were varied in order to minimize the normalized root-mean-square residual for the fit between the experimental and simulated  $I_t(\chi, \phi)$  data, with all other parameters fixed.<sup>24</sup> Good-quality fits to the experimental data were obtained at all temperatures (Figure 3; Table 1). In all plots of the experimental data, normalized transmitted X-ray intensity is shown.

Full characterization of the X-ray birefringence from a single crystal of BrCH/thiourea is contained in the experimental  $I_t(\chi, \phi)$  data, recorded as discussed above. For the HT phase, no significant variation in  $I_t(\chi, \phi)$  as a function of  $\chi$  and/or  $\phi$  is expected or observed, as a consequence of the essentially isotropic nature of the orientational distribution of the C–Br bonds in this phase, and the measured intensity is negligible for all crystal orientations. The  $I_t(\chi, \phi)$  data for several temper-



**Table 1.** Parameters Giving the Best Fit between Simulated and Experimental X-ray Birefringence Data at Each Temperature Studied in the LT Phase of BrCH/Thiourea<sup>a</sup>

T/K	<i>p</i>	$\psi/^\circ$	$\omega/^\circ$	R
200	0.33	60.2	5.0	0.009
160	0.54	55.1	4.8	0.015
130	0.67	54.0	5.0	0.021
100	0.78	53.7	5.0	0.028

<sup>a</sup>The normalized root-mean-square residual for the final fit between experimental and simulated data is denoted R.

atures (200, 160, 130, 100 K) in the LT phase are shown in Figure 3, left side. It is immediately obvious from these data that the X-ray birefringence changes substantially as a function of temperature within the LT phase.

Quantitative analysis of the data (including the temperature dependence) is discussed in detail below, but initially, it is instructive to gain qualitative insights into the X-ray birefringence behavior by considering separately the dependence of  $I_t$  on crystal orientation angle  $\chi$  with  $\varphi$  fixed (Figure 4a, recorded at  $\varphi = 0^\circ$ ) and on crystal orientation angle  $\varphi$  with  $\chi$  fixed (Figure 4b, recorded at  $\chi = -10^\circ$ ). These measurements effectively represent one-dimensional sections through the experimental  $I_t(\chi, \varphi)$  data shown in Figure 3 (although, as discussed above, they were actually measured independently of the data shown in Figure 3).

In the HT phase (270 K), there is no significant variation in  $I_t$  as a function of either  $\chi$  (black trace in Figure 4a) or  $\varphi$  (black trace in Figure 4b), reflecting the essentially isotropic orientational distribution of the BrCH guest molecules (and hence the C–Br bonds) in the HT phase. Thus, the crystal does not exhibit any significant X-ray birefringence in the HT phase.

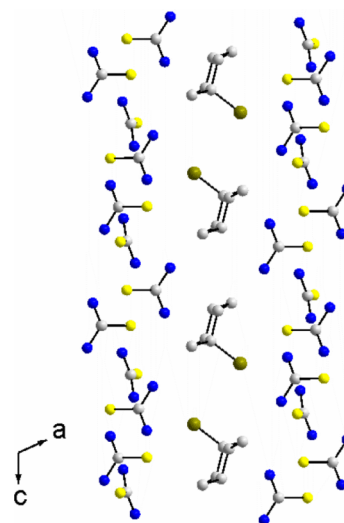
However, the behavior in the LT phase is dramatically different. Focusing initially at the lowest temperature studied (100 K), it is clear that  $I_t$  varies significantly as a function of both  $\chi$  (red trace in Figure 4a) and  $\varphi$  (red trace in Figure 4b), indicating a significant increase in the degree of orientational ordering of the C–Br bonds of the BrCH guest molecules in the LT phase. Within the range of  $\chi$  probed in Figure 4a, two maxima in  $I_t$  are observed, separated from each other by  $\Delta\chi = 90^\circ$  and each separated from the intervening minimum by  $\Delta\chi = 45^\circ$ , as expected from the analogy to optical birefringence. At 100 K,  $I_t$  also varies significantly as a function of  $\varphi$ , with minima observed at  $\varphi \approx -100$  and  $80^\circ$  within the range of  $\varphi$  probed. This behavior (with minima separated by  $\Delta\varphi = 180^\circ$ ) is entirely consistent with a material comprising a single orientational domain of the BrCH guest molecules, in which the C–Br bonds are *not* oriented along the *c*-axis (if the C–Br bonds were oriented along the *c*-axis, the transmitted intensity would be independent of  $\varphi$ , as observed previously<sup>7</sup> for 1-bromoadamantane/thiourea).

Now, considering the results at different temperatures within the LT phase, it is clear that  $I_t$  increases gradually as temperature is decreased but with no significant change in the values of  $\chi$  and  $\varphi$  that correspond to maxima and minima in  $I_t$  (Figure 4a and 4b). These observations suggest that the degree of ordering of the BrCH guest molecules increases as temperature is decreased but that the resultant orientation of the C–Br bonds does not vary significantly with temperature.

To understand the orientational properties in quantitative detail, it is necessary to consider the complete data of  $I_t$  as a

function of both crystal orientation angles  $\chi$  and  $\varphi$ . The experimental  $I_t(\chi, \varphi)$  data (Figure 3, left side) for the LT phase have been fitted using the theoretical model described above, allowing the resultant orientation of the C–Br bonds of the BrCH guest molecules relative to the unit cell axes (described by the angles  $\psi$  and  $\omega$ , defined in Figure 2b) to be determined as a function of temperature. The results of the fitting procedure (Figure 3) reveal very close agreement between experimental and simulated data at each temperature studied. Inter alia, the high quality of fits obtained provides support for the validity of the theoretical model, including our assumption that the X-ray birefringence data are dominated by a single orientational domain of the guest molecules.

The values of the structural parameters ( $\psi$  and  $\omega$ ) and the molecular polarization factor *p* determined from the fitting procedure are shown in Table 1. At 100 K, the orientation of the C–Br bond relative to the unit cell axes determined from the X-ray birefringence data is  $\psi = 53.7^\circ$  and  $\omega = 5.0^\circ$ , in very close agreement with the corresponding geometric information ( $\psi = 52.5^\circ$  and  $\omega = 3.5^\circ$  at 110 K; Figure 5)<sup>27</sup> established from

**Figure 5.** Crystal structure of BrCH/thiourea determined at 110 K, viewed perpendicular to the tunnel axis, showing that the C–Br bonds of all BrCH guest molecules form a bond-tilt angle of  $\sim 52.5^\circ$  with respect to the tunnel axis (vertical). Hydrogen atoms are omitted for clarity.

an independent single-crystal XRD study.<sup>10</sup> Although the errors in the values of  $\psi$  and  $\omega$  extracted from fitting the X-ray birefringence data are negligibly small (of the order of  $0.001^\circ$ ), systematic errors in these values (primarily arising from establishing the orientation of the crystallographic axes relative to the laboratory reference frame) are significantly larger (estimated to be about  $\pm 1^\circ$ ). The estimated errors in the values determined from single-crystal XRD are  $\pm 0.6^\circ$ .

At the other temperatures studied in the LT phase (200, 160, 130 K), there is also excellent agreement between the experimental and best-fit simulated X-ray birefringence data (Figure 3). The results reveal a small (but systematic) variation in the bond tilt angle  $\psi$  as a function of temperature, whereas the bond azimuthal angle  $\omega$  shows no significant temperature dependence. The fitted value of the molecular polarization factor *p* increases monotonically (and almost linearly) as temperature is decreased.

To explore the temperature dependence of the X-ray birefringence in more detail (and thus to gain insights into the process of ordering of the BrCH guest molecules within the LT phase), the transmitted X-ray intensity was recorded as a detailed function of temperature between 100 and 270 K, with the crystal orientation fixed at  $\chi = -10^\circ$  and  $\varphi = 0^\circ$  [i.e., the orientation corresponding to the global maximum in  $I_t(\chi, \varphi)$ ; see Figure 3]. It is informative to display the results (Figure 6)

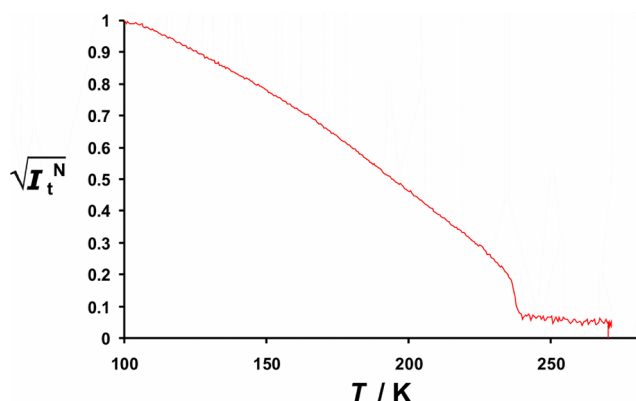


**Figure 6.** Square root of the normalized transmitted X-ray intensity  $(I_t^N)^{1/2}$  for a single crystal of BrCH/thiourea as a function of temperature for the specific crystal orientation with  $\chi = -10^\circ$  and  $\varphi = 0^\circ$ .

as the square root of the normalized transmitted intensity  $(I_t^N)^{1/2}$  versus temperature, recognizing<sup>7</sup> that  $(I_t^N)^{1/2}$  scales with the molecular polarization factor  $p$ . It is clear from Figure 6 that the behavior in the HT phase is essentially independent of temperature.<sup>28</sup> At the phase transition temperature (233 K), the transmitted intensity increases by only a small step, but below the phase transition temperature, the transmitted intensity increases substantially, with an almost linear increase in  $(I_t^N)^{1/2}$ , as temperature decreases toward 100 K within the LT phase.

Our observations suggest that only a relatively minor increase in the degree of ordering of the BrCH guest molecules occurs at the phase transition temperature (even though there is a change in crystal symmetry and a discontinuity in the unit cell volume of the thiourea host structure at the phase transition temperature;<sup>10</sup> see Figure 1), but a much more substantial increase in the degree of orientational ordering of the guest molecules occurs in a gradual and progressive manner as temperature is decreased below the phase transition temperature. In contrast, in the case of a transformation from a completely isotropic state in the HT phase to a completely orientationally ordered state in the LT phase, the X-ray birefringence signal would exhibit a substantial jump at the phase transition temperature (in principle, corresponding to a jump in the value of the molecular polarization factor from  $p \approx 0$  to  $p \approx 1$ ), with no significant variation on decreasing temperature within the LT phase.

Our conclusion from the X-ray birefringence results that the orientational ordering of the BrCH guest molecules occurs progressively as temperature is decreased within the LT phase is in agreement with independent results from single-crystal XRD<sup>10</sup> and solid-state NMR.<sup>12,14,15</sup> A study of the dynamic properties of the BrCH guest molecules by solid-state  $^{13}\text{C}$  and  $^2\text{H}$  NMR<sup>15</sup> between 350 and 100 K concluded that rapid ring inversion and essentially unrestricted reorientation of the whole

molecule relative to the host structure occur in the HT phase, while in the higher-temperature region of the LT phase, restricted but rapid motion of the BrCH guest molecules still occurs. However, at  $\sim 110$  K and lower temperatures, rigid-limit NMR spectra were observed, indicating that the reorientational motions of the guest molecules become frozen in this temperature regime. Structure determination calculations from single-crystal XRD data<sup>10</sup> also concur with this picture as well-defined localization of the positions and orientations of the BrCH guest molecules could be identified only at 110 K. At higher temperatures in the LT phase, the precision of the refined guest substructure was found to decrease significantly as temperature increased, reflecting an increased degree of disorder such that a satisfactory description of the guest substructure could not be obtained, even with refinement of large anisotropic displacement parameters to subsume the effects of the disorder.

As suggested by our X-ray birefringence results, a process of progressive ordering of the guest molecules occurs as temperature is decreased within the LT phase due to a gradual reduction in the dynamics of the guest molecules, which gradually assemble into a preferred orientation within the host tunnel as their mobility decreases and as the host tunnel contracts. Our observations are fully consistent with the idea that the ensemble of orientations of the C–Br bond directions in the LT phase represents a distribution about a specific preferred orientation. Furthermore, as temperature is decreased within the LT phase, this distribution becomes narrower (reflected by a gradual increase in the molecular polarization factor  $p$ ), while the actual preferred orientation (characterized by the values of  $\psi$  and  $\omega$ ) exhibits only minor changes as a function of temperature (primarily involving a slight decrease in the bond tilt angle  $\psi$ ; Table 1). It is noteworthy that, while the structural results from X-ray birefringence at the lowest temperature studied (100 K) correlate very well with the information determined from single-crystal XRD in the same temperature regime (110 K), our X-ray birefringence data provide more detailed insights into the overall directional properties of the C–Br bonds than those obtained from single-crystal XRD in the higher-temperature regions of the LT phase (more details of which, including the behavior of anisotropic displacement parameters as a function of temperature, are given in ref 10).

Our results demonstrate clearly that X-ray birefringence is a reliable and widely applicable strategy for probing the orientational properties of specific bonds in solids, as demonstrated here in relation to the process of progressive molecular orientational ordering that occurs below the solid-state phase transition in the BrCH/thiourea inclusion compound. This work paves the way for the sensitivity and versatility of X-ray birefringence to be exploited in the future as a technique for determining bond orientational distributions in a wide range of other types of anisotropic material. Examples of areas for future application include characterization of order–disorder phase transitions in other solid inclusion compounds (for which the chlorocyclohexane/thiourea inclusion compound<sup>29</sup> would provide interesting contrasts to the results reported here for BrCH/thiourea) and other rotator-phase solids, as well as determination of the anisotropic distributions of bond orientations in amorphous solids, liquid-crystalline phases, and molecular materials that undergo ferroelectric or ferroelastic phase transitions. Furthermore, similar strategies may also be exploited to study bond orientations of molecules

present within thin films<sup>30</sup> or molecules adsorbed on solid surfaces.

Finally, it is relevant to note that to obtain good fits to the experimental X-ray birefringence data, we found that a small degree of circular polarization of the incident X-ray beam must be incorporated into the model<sup>31</sup> (the value  $P_2 = -0.075$  was extracted from each individual data set<sup>24</sup>). From this observation, we suggest that this type of measurement is so sensitive to the circular polarization that it could form the basis of a very simple and effective polarimeter.

## AUTHOR INFORMATION

### Corresponding Author

\*E-mail: HarrisKDM@cardiff.ac.uk.

### Notes

The authors declare no competing financial interest.

## ACKNOWLEDGMENTS

We are grateful to Diamond Light Source for the award of beam time for experiments on beamline B16. We thank EPSRC (studentships to B.A.P., G.R.E.-G., and A.M.-R.) and Cardiff University for financial support.

## REFERENCES

- (1) Born, M.; Wolf, E. *Principles of Optics*, 7th ed.; Cambridge University Press: Cambridge, U.K., 1999.
- (2) Hartshorne, N. H.; Stuart, A. *Practical Optical Crystallography*, 2nd ed; Edward Arnold Publishers Ltd.: London, U.K., 1969.
- (3) Kaminsky, W.; Claborn, K.; Kahr, B. Polarimetric Imaging of Crystals. *Chem. Soc. Rev.* **2004**, 33, 514–525.
- (4) Sauvage, M.; Malgrange, C.; Petroff, J.-F. Rotatory Power Measurements in the X-ray Range with Synchrotron Radiation: Experimental Set-Up and Preliminary Results for NaBrO<sub>3</sub> Single Crystals. *J. Appl. Crystallogr.* **1983**, 16, 14–20.
- (5) Okitsu, K.; Oguchi, T.; Maruyama, H.; Amemiya, Y. Faraday Effect and X-ray Birefringence at Cobalt K-Absorption Edge with the Tunable X-ray Polarimeter. *Proc. Soc. Photo- Opt. Instrum. Eng.* **1996**, 2873, 100–104.
- (6) Mertins, H.-C.; Oppeneer, P. M.; Valencia, S.; Gudat, W.; Senf, F.; Bressler, P. R. X-ray Natural Birefringence in Reflection from Graphite. *Phys. Rev. B* **2004**, 70, 235106.
- (7) Palmer, B. A.; Morte-Ródenas, A.; Kariuki, B. M.; Harris, K. D. M.; Collins, S. P. X-ray Birefringence from a Model Anisotropic Crystal. *J. Phys. Chem. Lett.* **2011**, 2, 2346–2351.
- (8) Chao, M.-H.; Kariuki, B. M.; Harris, K. D. M.; Collins, S. P.; Laundry, D. Design of a Solid Inclusion Compound with Optimal Properties as a Linear Dichroic Filter for X-ray Polarization Analysis. *Angew. Chem., Int. Ed.* **2003**, 42, 2982–2985.
- (9) Ishibashi, T.; Machida, M.; Koyano, N. Structure of Inclusion Compound C<sub>6</sub>H<sub>11</sub>Br/SC(NH<sub>2</sub>)<sub>2</sub> Studied by X-ray Diffraction. *J. Korean Phys. Soc.* **2005**, 46, 228–231.
- (10) Palmer, B. A.; Kariuki, B. M.; Morte-Ródenas, A.; Harris, K. D. M. Structural Rationalization of the Phase Transition Behavior in a Solid Organic Inclusion Compound: Bromocyclohexane/Thiourea. *Cryst. Growth Des.* **2012**, 12, 577–582.
- (11) McKinnon, M. S.; Wasylishen, R. E. A <sup>13</sup>C CP/MAS NMR Investigation of the Conformation of Substituted Cyclohexanes in Thiourea Inclusion Compounds. *Chem. Phys. Lett.* **1986**, 130, 565–568.
- (12) Müller, K. <sup>13</sup>C Magic Angle Spinning NMR Investigations of Thiourea Inclusion Compounds. *Magn. Reson. Chem.* **1992**, 30, 228–234.
- (13) Aliev, A. E.; Harris, K. D. M. Conformational Properties of Monosubstituted Cyclohexanes in their Thiourea Inclusion Compounds and in Solution: Variable-Temperature One-Dimensional and

Two-Dimensional <sup>13</sup>C NMR Investigations. *J. Am. Chem. Soc.* **1993**, 115, 6369–6377.

(14) Müller, K. Solid-State <sup>13</sup>C NMR Investigations of Monosubstituted Cyclohexanes in Thiourea Inclusion Compounds. *Magn. Reson. Chem.* **1995**, 33, 113–123.

(15) Ternieden, S.; Müller, K. Solid State NMR Studies of the Bromocyclohexane/Thiourea Inclusion Compound. *J. Inclusion Phenom. Mol. Recognit. Chem.* **1998**, 30, 289–308.

(16) Allen, A.; Fawcett, V.; Long, D. A. Raman Spectroscopic Investigation of Conformation of Cyclohexyl Halides C<sub>6</sub>H<sub>11</sub>X (X = Cl, Br and I) in Thiourea Clathrates. *J. Raman Spectrosc.* **1976**, 4, 285–294.

(17) Shannon, I. J.; Jones, M. J.; Harris, K. D. M.; Siddiqui, M. R. H.; Joyner, R. W. Probing the Conformational Properties of Guest Molecules in Solid Inclusion Compounds via EXAFS Spectroscopy: Bromine K-Edge EXAFS Studies of the Bromocyclohexane/Thiourea and *trans*-1-Bromo-2-chlorocyclohexane/Thiourea Inclusion Compounds. *J. Chem. Soc., Faraday Trans.* **1995**, 91, 1497–1501.

(18) Lenné, H.-U. Röntgenographische Strukturuntersuchungen Hexagonaler Einschlussverbindungen des Thioharnstoffs. *Acta Crystallogr.* **1954**, 7, 1–15.

(19) Hough, E.; Nicholson, G. X-ray Crystallographic Studies on Ferrocene Included in a Thiourea Host Lattice. *J. Chem. Soc., Dalton Trans.* **1978**, 1, 15–18.

(20) Gopal, R.; Roberston, B. E.; Rutherford, J. S. Adamantane Inclusion Complexes with Thiourea and Selenourea. *Acta Crystallogr., Sect. C* **1989**, 45, 257–259.

(21) Harris, K. D. M.; Thomas, J. M. Structural Aspects of the Chlorocyclohexane/Thiourea Inclusion System. *J. Chem. Soc., Faraday Trans.* **1990**, 86, 1095–1101.

(22) Crystals of the BrCH/thiourea inclusion compound were prepared by cooling a solution of thiourea and BrCH (~3:1 molar ratio) in methanol from 55 to 20 °C over ~29 h. The crystals were needle-shaped, with the needle axis corresponding to the tunnel direction (*c*-axis). Powder XRD confirmed that the product was a monophasic sample of a conventional thiourea inclusion compound.

(23) The same type of measurement recorded on the first cooling cycle indicated that there are no significant differences in the X-ray birefringence behavior upon cooling and warming the crystal.

(24) The theoretical model for simulating the  $I_i(\chi, \varphi)$  data assumes that the crystal exhibits uniaxial anisotropy with the optic axis along the direction of the C–Br bond and is based on the theoretical framework elaborated in ref 7 (see also the Electronic Supporting Information for ref 7). For this reason, we do not reiterate the underlying theory here. As discussed in the text, it is convenient in the present work to use the angles  $\psi$  and  $\omega$  (defined in Figure 2b) to describe the orientation of the C–Br bond of the BrCH guest molecules relative to the crystallographic axes of the thiourea host structure and to use the angles  $\chi$  and  $\varphi$  (defined in Figure 2a) to describe the orientation of the crystallographic axes of the thiourea host structure relative to the laboratory reference frame, and the model was modified accordingly in the present work. Following the description of the model in ref 7, the simulated  $I_i(\chi, \varphi)$  data depend on the following parameters: (i) molecular polarization factor  $p$ , (ii) bond tilt angle  $\psi$ , (iii) bond azimuthal angle  $\omega$ , (iv) ratio of birefringence to dichroism,  $\Delta\gamma''/\Delta\gamma' = 1.0$  (value estimated from ref 7), (v) ratio of dichroism to isotropic absorption,  $\Delta\gamma'/\Delta\gamma = 0.58$  (value estimated from ref 7), (vi) isotropic absorption,  $\gamma t = 1.2$  (measured value), (vii) scattering angle for the polarization analyzer [graphite (0, 0, 10)],  $2\theta = 86.3^\circ$ , (viii) polarization analyzer rotation angle,  $\eta = 89^\circ$  (nominally  $90^\circ$ , but a better fit was obtained for  $89^\circ$ ), (ix) Stokes parameter for linear polarization at  $45^\circ$  from horizontal,  $P_1 = 0$  (the expected value of  $P_1$ ), (x) Stokes parameter for circular polarization,  $P_2 = -0.075$  (nominally  $P_2 = 0$ , but a small deviation may arise as discussed in ref 31), and (xi) Stokes parameter for horizontal linear polarization,  $P_3 = 0.99$  (nominally  $P_3 = 1$ , but a small reduction is expected due to electron beam size and X-ray beam divergence). In the least-squares fitting procedure, different sets of parameters were handled in different ways. In the final fitting procedure, only the

parameters  $p$ ,  $\psi$ , and  $\omega$  were allowed to vary (the values corresponding to the best fit at each temperature are given in Table 1). The other parameters were fixed at values (quoted above) known independently (in the case of  $\Delta\gamma''/\Delta\gamma'$ ,  $\Delta\gamma'/\Delta\gamma$ ,  $\gamma t$ ,  $2\theta$ , and  $P_1$ ) or were fixed at values (also quoted above) established from preliminary fits to the data (in the case of  $P_2$ ,  $P_3$ , and the overall scale factor at each temperature). As mentioned in the text, the quality of fit was found to be insensitive to variation of these parameters, hence justifying our strategy of fixing them in order to keep the total number of fitted parameters as low as justifiably possible.

(25) Assuming uniaxial symmetry, X-ray birefringence (as in the case of linear X-ray dichroism<sup>26</sup>) scales with the  $Q_{zz}$  component of the atomic quadrupole moment of the relevant orbital for the X-ray transition (in the present case involving the bromine 4p shell via the  $\sigma^*$  antibonding orbital associated with the C–Br bond). Clearly, the ensemble average of the quadrupole moment of all molecules in the sample depends on the orientational distribution of the C–Br bonds and is described by the parameter  $p$ , which is in the range of  $0 \leq p \leq 1$ . The limit  $p = 0$  arises for an isotropic orientational distribution, whereas the limit  $p = 1$  arises for a fully polarized system. We note that as the molecular polarization factor  $p$  depends on the electric quadrupole moment, it is parity even and therefore does not vanish in the case of a centrosymmetric crystal.

(26) van der Laan, G.; Schofield, P. F.; Cressey, G.; Henderson, C. M. B. Natural Linear Dichroism at the Fe 2p Absorption Edge of Gillespite. *Chem. Phys. Lett.* **1996**, 252, 272–276.

(27) In the present context, we make the reasonable assumption that the X-ray birefringence is dominated by the major guest orientation established from single-crystal XRD.

(28) We note that the value of  $(I_t^N)^{1/2}$  does not actually vanish in the high-temperature phase (despite the isotropic distribution of C–Br bond orientations) as a consequence of the fact that the polarization analyzer rotation angle was not exactly  $90^\circ$ .

(29) Soetens, J.-C.; Desmedt, A.; Guillaume, F.; Harris, K. D. M. Molecular Dynamics Simulation Study of Cyclohexane Guest Molecules in the Cyclohexane/Thiourea Inclusion Compound. *Chem. Phys.* **2000**, 261, 125–135.

(30) In this regard, it is relevant to highlight a very recent paper reporting the use of polarized X-rays to probe orientational ordering in organic films; see: Collins, B. A.; Cochran, J. E.; Yan, H.; Gann, E.; Hub, C.; Fink, R.; Wang, C.; Schuettfort, T.; McNeill, C. R.; Chabiny, M. L.; Ade, H. Polarized X-ray Scattering Reveals Non-Crystalline Orientational Ordering in Organic Films. *Nat. Mater.* **2012**, 11, 536–543.

(31) A modest circular component to the beam polarization is not surprising and may be caused by a small vertical misalignment of the slits that define the emission from the bending magnet radiation source.